

Genetic Unmasking of an Epigenetically Silenced microRNA in Human Cancer Cells

Amaia Lujambio,¹ Santiago Ropero,¹ Esteban Ballestar,¹ Mario F. Fraga,¹ Celia Cerrato,³ Fernando Setién,¹ Sara Casado,¹ Ana Suarez-Gauthier,² Montserrat Sanchez-Cespedes,² Anna Gitt,⁴ Inmaculada Spiteri,⁴ Partha P. Das,⁵ Carlos Caldas,⁴ Eric Miska,⁵ and Manel Esteller¹

¹Cancer Epigenetics Laboratory and ²Lung Cancer Laboratory, Spanish National Cancer Centre (CNIO), Madrid, Spain; ³Centre de Regulació Genòmica, Universitat Pompeu Fabra, Barcelona, Catalonia, Spain; ⁴Cancer Genomics Program, Department of Oncology, Hutchison-Medical Research Council Research Centre; and ⁵Wellcome Trust/Cancer Research UK Gurdon Institute and Department of Biochemistry, University of Cambridge, Cambridge, United Kingdom

Abstract

The mechanisms underlying microRNA (miRNA) disruption in human disease are poorly understood. In cancer cells, the transcriptional silencing of tumor suppressor genes by CpG island promoter hypermethylation has emerged as a common hallmark. We wondered if the same epigenetic disruption can “hit” miRNAs in transformed cells. To address this issue, we have used cancer cells genetically deficient for the DNA methyltransferase enzymes in combination with a miRNA expression profiling. We have observed that DNA hypomethylation induces a release of miRNA silencing in cancer cells. One of the main targets is miRNA-124a, which undergoes transcriptional inactivation by CpG island hypermethylation in human tumors from different cell types. Interestingly, we functionally link the epigenetic loss of miRNA-124a with the activation of cyclin D kinase 6, a bona fide oncogenic factor, and the phosphorylation of the *retinoblastoma*, a tumor suppressor gene. [Cancer Res 2007;67(4):1424–9]

Introduction

microRNAs (miRNA) are short, 22-nucleotide, noncoding RNAs that are thought to regulate gene expression by sequence-specific base pairing in the 3'-untranslated regions (UTR) of the target mRNA, inducing direct mRNA degradation or translational inhibition (1, 2). miRNA expression patterns can be developmentally regulated, tissue specific, or steadily expressed in the whole organism (1, 2) and are considered to play important roles in cell proliferation, apoptosis, and differentiation (1, 2). In disease, recent studies have shown that miRNA expression profiles are distinct between normal tissues and derived tumors (3) and between different tumor types (3). Interestingly, down-regulation of subsets of miRNAs is a common finding in many of these studies (2, 3), suggesting that some of these miRNAs may act as putative tumor suppressor genes. This last indication has been studied in more detail for particular cases, and for example, the down-regulated let-7, miR-15/miR-16, and miR-127 target the oncogenic factors RAS, BCL-2, and BCL-6, respectively (4–6). One explanation is a failure at the posttranscriptional regulation of these miRNAs in

cancer cells (7). However, additional mechanisms could also be invoked. Because the down-regulation of many relevant tumor suppressor genes in human cancer, such as *hMLH1*, *BRCA1*, and *p16INK4a*, has been tightly linked to the presence of CpG island promoter hypermethylation (8–10), we wondered if the same mechanism could be playing a role in the described loss of miRNA expression in tumors. In this regard, restoration of miRNA-127 expression in cancer cells by treatment with a DNA-demethylating agent has been recently reported (6). These recent and exciting data support the idea of an aberrant DNA methylation pattern of miRNA genomic loci in human tumors.

To explore the putative presence of DNA methylation-associated silencing of miRNAs in cancer cells, we used a genetic approach. We compared the miRNA expression profile of the wild-type colon cancer cell line HCT-116 with the same cell line after genetic disruption by homologous recombination of DNA methyltransferase 1 (DNMT1) and DNMT3b (double knockout, DKO; ref. 11), using a miRNA microarray expression profiling method (12). DKO cells show a drastic reduction of DNMT activity, 5-methylcytosine DNA content, and, most important, a release of gene silencing associated with CpG island hypomethylation (11, 13). Our results prove that DNA hypermethylation contributes to the transcriptional down-regulation of miRNAs in human tumors, and that the epigenetic silencing of miR-124a in cancer cells modulate the activity of oncogenes [cyclin D kinase 6 (CDK6)] and tumor suppressor genes [*retinoblastoma* (*Rb*)].

Materials and Methods

Human cancer cell lines and primary tumor samples. HCT-116 colon cancer cells and double DNMT1^{-/-}DNMT3b^{-/-} (DKO) cells were grown as previously described (11). HCT-116 cells were treated with 5-aza-2-deoxycytidine (1 μmol/L) for 72 h. HCT-116 and DKO cells were a generous gift from Dr. Bert Vogelstein (Johns Hopkins Kimmel Comprehensive Cancer Center, Baltimore, MD). All the other human cancer cell lines (*n* = 30) were obtained from the American Type Culture Collection (Rockville, MD). Primary tumor samples (*n* = 208) and corresponding normal tissues (*n* = 22) from different cell types were obtained at the time of clinically indicated procedures.

RNA isolation and miRNA expression analysis. Total RNA was isolated from HCT-116 and DKO cells by Trizol (Invitrogen, San Diego, CA) extraction according to the manufacturer's instructions. miRNA microarray profiling was done as described (12). In brief, 5 μg of total RNA was used for each hybridization. miRNA expression levels were normalized by three different artificial miRNA spikes. Microarray probes were oligonucleotides with sequences complementary to miRNAs. Printing and hybridization were done using the protocols from the slide manufacturer.

DNA methylation analyses. The CpG Island Searcher Program (14) was used to determine which miRNAs were embedded in a CpG island. The

Note: Supplementary data for this article are available at Cancer Research Online (<http://cancerres.aacrjournals.org/>).

Requests for reprints: Manel Esteller, Cancer Epigenetics Laboratory, Spanish National Cancer Centre (CNIO), Melchor Fernandez Almagro 3, 28029 Madrid, Spain. Phone: 34-91-2246949; Fax: 34-91-2246923; E-mail: mesteller@cnio.es.

©2007 American Association for Cancer Research.
doi:10.1158/0008-5472.CAN-06-4218

DNA methylation status was established by PCR analysis of bisulfite-modified genomic DNA, which induces chemical conversion of unmethylated, but not methylated, cytosine to uracil, using two procedures. First, methylation status was analyzed by bisulfite genomic sequencing of both strands of the corresponding CpG islands. The second analysis used methylation-specific PCR using primers specific for either the methylated or modified unmethylated DNA. The primers used are described in Supplementary Table S1.

Rapid amplification of cDNA ends. The 5' rapid amplification of cDNA ends (RACE) system was done using Invitrogen kit and according to the manufacturer's instruction. Briefly, 5 μ g of brain total RNA was reverse transcribed into cDNA using SuperScript II RT reverse transcriptase and specific reverse primers (GSP1). After that, cDNAs were amplified by PCR

using Elongase Amplification System (Invitrogen) and other specific primers (GSP2 or GSP3 for nested amplification in the cases of miR-124a1 and miR-124a2). The PCR primers are described in Supplementary Table S1.

Reverse transcription-PCR and quantitative reverse transcription-PCR for miRNAs. We used conventional and quantitative-real-time reverse transcription-PCR (RT-PCR) to measure miRNA expression. The primers used are described in Supplementary Table S1. For RT-PCR, glyceraldehyde-3-phosphate dehydrogenase was used as internal control. PCR products were analyzed in a 3% agarose gel. Real-time PCR analysis of miRNAs was done as previously described (15). The real-time PCR reactions typically contained 5 pmol of the gene-specific primer, 5 pmol of the common antisense oligonucleotide, 10 μ L SYBR Green PCR Master Mix (Applied

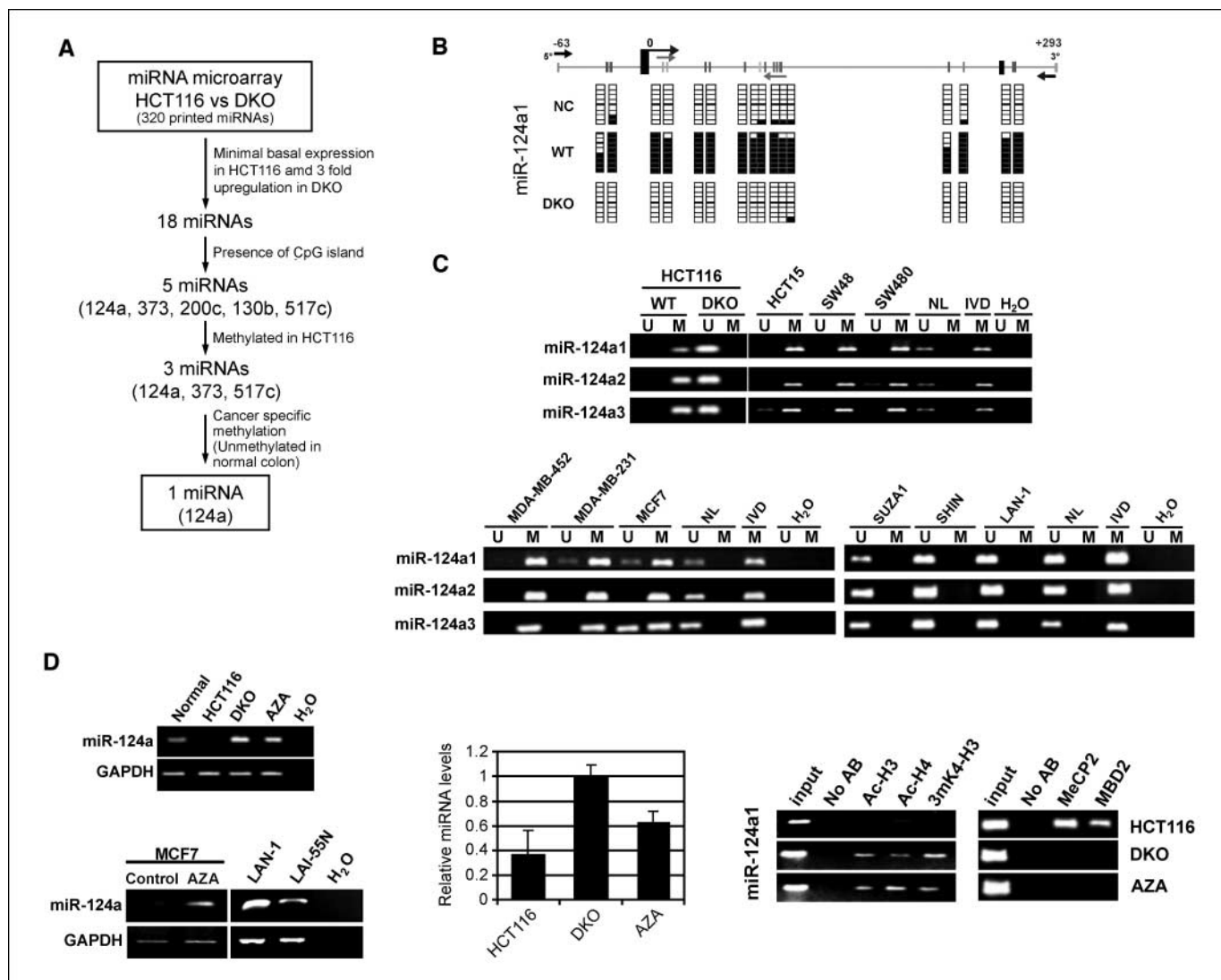


Figure 1. Epigenetic silencing of miR-124a in cancer cells. **A**, schematic strategy used to unmask DNA methylation-associated repression of miRNAs in colon cancer cells. **B**, bisulfite genomic analyses of miR-124a CpG island methylation status in normal colon, HCT-116, and DKO cells. Eight single clones are represented for each sample. Unmethylated (white squares) and methylated (black squares) CpGs. Location of the sequencing (black arrow) and methylation-specific PCR primers (gray arrow). Transcription start site (thick arrow). **C**, methylation-specific PCR analyses for miR-124a methylation in human cancer cell lines. Unmethylated (U) or methylated (M) sequences. Normal lymphocytes (NL) and *in vitro* methylated DNA (IVD) are shown as negative and positive controls for unmethylated and methylated sequences, respectively. **D**, expression analyses of precursor (left column) and mature (middle column) miR-124a by conventional RT-PCR or quantitative RT-PCR, respectively. The miR-124a methylated HCT-116 and MCF7 cells, treated with the DNA-demethylating agent 5-aza-2'-deoxycytidine (AZA), and DKO cells show miR-124a up-regulation. Two unmethylated neuroblastoma cell lines (LAN-1 and LAI-55N) show miR-124a basal expression. Right column, chromatin immunoprecipitation assay for histone modification marks and methyl-CpG binding domain proteins (MeCP2 and MBD2) in the miR-124a CpG island. The presence of miR-124a CpG island methylation is associated with the lack of histone modifications linked to transcriptional activity (acetylation of histones H3 and H4 and trimethylation of Lys⁴ of histone H3) and with the occupancy by MBDs, whereas the opposite scenario is observed when DNA demethylation events are present by genetic disruption of the DNMTs (DKO cells) or pharmacologic treatment with a DNA-demethylating agent (5-aza-2'-deoxycytidine).

Table 1. Profile of miR-124a methylation in human cancer cell lines and primary tumors

A.

	Tissue (cell lines and control samples)														
	Colon				Breast				Neuroblastoma						
	HCT116	HCT15	SW48	SW480	COLO205	RKO	LOVO	MDA-MB-231	MCF7	MDA-MB-453	LAI-55N	SHIN	IMR-32	SK-N-AS	LAN-1
miR-124a1	[Black square]				[Black square]				[Black square]			[Black square]			
miR-124a2	[Black square]				[Black square]				[Black square]			[Black square]			
miR-124a3	[Black square]				[Black square]				[Black square]			[Black square]			

B.

Tissue type	Hypermethylated samples (n = 208)
Colon	42/56 (75%)
Breast	7/22 (32%)
Lung	13/27 (48%)
Leukemia	14/39 (36%)
Lymphoma	11/27 (41%)
Neuroblastoma	0/22 (0%)
Sarcoma	0/15 (0%)

NOTE: Black and gray squares indicate methylated and unmethylated miR-124a, respectively.

Biosystems, Foster City, CA), and 6 µL of the diluted cDNAs in a total volume of 20 µL.

Chromatin immunoprecipitation assay. Standard chromatin immunoprecipitation assays were done as previously described (16). In brief, cells were treated with 1% formaldehyde for 15 min. Then, chromatin was sheared with a Bioruptor (Diagenode, Philadelphia, PA) to an average length of 0.4 to 0.8 kb for this analysis. The following antibodies were used: anti-MeCP2 (ab3752), anti-MBD2 (ab3754), and anti-trimethyl-K4 histone H3 (ab8580/ab1220; Abcam, Cambridge, MA) and anti-acetyl H3 (06-599) and anti-acetyl H4 (06-598; Upstate Biotechnologies, Lake Placid, NY). PCR amplification was done in 20 µL with specific primers for each of the analyzed promoters. Primers used are described in Supplementary Table S1.

Databases and Genbank accession number. The miRNA sequences were analyzed using miRBase⁶ and University of California at Santa Cruz Human Genome Browser⁷. Information of base pairing comparison between miR-124a and its target site in the 3'-UTR of CDK6 mRNA is available at Human miRNA Targets⁸ and miRBase Targets.⁶

Analyses of CDK6 and phosphorylated Rb expression by Western blot, immunohistochemistry, and RT-PCR. Western blot was done as previously described (16). The membranes were immunoprobed with antibodies against CDK6 (1:1,000; Cell Signaling, Temecula, CA) and P-Rb-S807/811 (1:1,000; Cell Signaling). An antibody to β-actin (1:5,000; Sigma, St. Louis, MO) was used as a loading control. Immunohistochemical staining of CDK6 and P-Rb-S807/811 was done using the above-described antibodies at a 1:1,500 dilution. For the RT-PCR of CDK6, total RNA (5 µg) was used for reverse transcription, using primers specific for CDK6 mRNA (Supplementary Table S1).

Transfection with miR-124a precursor molecules and luciferase assays. miR-124a precursor molecules and negative control miRNA were

purchased from Ambion (Austin, TX). Experiments involving transient transfections of miRNAs were carried out with oligofectamine (Invitrogen) using 100 nmol/L RNA duplexes. The cells were collected 48 h after transfection, and the expression of CDK6 and P-Rb-S807/811 was analyzed

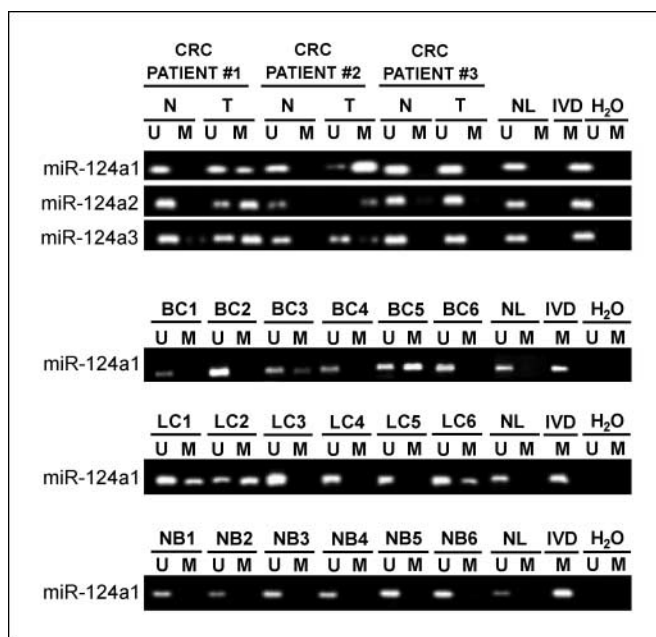


Figure 2. Methylation-specific PCR analyses for miR-124a methylation in primary human tumors. Unmethylated (U) or methylated (M) sequences. Normal lymphocytes (NL) and *in vitro* methylated DNA (IVD) are shown as unmethylated and methylated control sequences, respectively. *Top*, pairs of normal colon versus colorectal tumors from three different patients. *Bottom*, methylation-specific PCR analyses for miR-124a methylation in primary breast (*top*), lung (*middle*), and neuroblastoma (*bottom*) tumors. CRC, colorectal cancer.

⁶ <http://microrna.sanger.ac.uk/>
⁷ <http://genome.cse.ucsc.edu/>
⁸ <http://www.microrna.org/>

Table 1. Profile of miR-124a methylation in human cancer cell lines and primary tumors (Cont'd)

A.	Tissue (cell lines and control samples)													
	Lymphoma			Leukemia				Sarcoma			Lung			
	KARPAS	RAJI	U-937	KG1a	REH	RS4;11	KOPN8	Hs 819.T	A673	H358	CALU3	A549	A427	H2126
miR-124a1	■			■				■			■			
miR-124a2	■			■				■			■			
miR-124a3	■			■				■			■			

by Western blot and RT-PCR. Luciferase constructs were made by ligating oligonucleotides containing the wild-type or mutant putative target site of the CDK6 3'-UTR into the multi-cloning site of the p-MIR Reporter Luciferase vector (Ambion). Cells were cotransfected using LipofectAMINE 2000 (Invitrogen) with 0.4 μ g of firefly luciferase reporter vector containing the wild-type or mutant oligonucleotides, 0.02 μ g pGal control vector, and 100 ng of miR-124a precursor. Luciferase activity was measured 48 h after transfection using β -galactosidase for normalization.

Results and Discussion

DNA methylation analyses of up-regulated miRNAs in cancer cells deficient in DNMTs. Our genetic screening revealed that 18 of the 320 human miRNAs printed in the microarray

showed minimal basal expression in wild-type HCT-116 cells and were up-regulated >3-fold in DKO cells (Fig. 1A). Of these significantly up-regulated miRNAs, five of them were embedded in a canonical CpG island (Fig. 1A). Bisulfite genomic sequencing analyses of multiple clones of the original HCT-116 cells showed dense CpG island hypermethylation for miRNA-124a, miRNA-517c, and miR-373 (Fig. 1B; Supplementary Fig. S1). Because we wanted to focus in the cancer-specific DNA methylation changes, we analyzed by bisulfite genomic sequencing the DNA methylation status of these miRNA in normal colon tissues ($n = 10$), to exclude tissue-specific methylation patterns. miRNA-517c and miRNA-373 were found to be densely methylated in normal colon tissues (Supplementary Fig. S1), whereas miR-124a-embedded

Figure 3. Epigenetic silencing of miR-124a leads to CDK6 activation. *A*, Western blot for CDK6 in wild-type HCT-116, HCT-116 cells treated with a DNA-demethylating agent (5-aza-2'-deoxycytidine), and DKO cells. These two cell lines show a reduction in CDK6 levels. RT-PCR analyses of CDK6 mRNA do not show any change. *B*, miR-124a interact and interfere with the 3'-UTR of CDK6 mRNA. *Top*, base pairing comparison between mature miR-124a and the wild-type (WT) or mutant (MUT) CDK6 putative target site. *Bottom*, luciferase assays of DKO (miR-124a expressor) or HCT-116 (miR-124a non-expressor) cells transfected with firefly luciferase constructs containing CDK6-WT or CDK6-MUT. In the case of HCT-116 cells, the results of miR-124a cotransfection are also shown. Normalized luciferase activities are represented. *C, top*, Western blots for CDK6 in original HCT-116 cells and HCT-116 cells transfected with miR-124a precursor, showing CDK6 down-regulation. RT-PCR analyses of CDK6 mRNA do not show any change. *Bottom*, Western blot for phosphorylated Rb shows that HCT-116 cells transfected with the miR-124a precursor, HCT-116 cells treated with the DNA-demethylating agent, and DKO cells are hypophosphorylated at the two Rb sites mediated by CDK6. *D*, immunohistochemistry of CDK6 and phosphorylated Rb in human primary lung tumors. *Left*, miR-124a unmethylated tumor showing loss of CDK6 expression and hypophosphorylated Rb; *right*, miR-124a methylated tumor showing strong CDK6 staining and phosphorylated Rb. Those tumors with a high percentage of tumor cells (>50%) with positive nuclear staining were considered to have strong CDK6 expression. *Bottom*, table representing the distribution of cases. *GAPDH*, glyceraldehyde-3-phosphate dehydrogenase.

Top, base pairing comparison between mature miR-124a and the wild-type (WT) or mutant (MUT) CDK6 putative target site. *Bottom*, luciferase assays of DKO (miR-124a expressor) or HCT-116 (miR-124a non-expressor) cells transfected with firefly luciferase constructs containing CDK6-WT or CDK6-MUT. In the case of HCT-116 cells, the results of miR-124a cotransfection are also shown. Normalized luciferase activities are represented. *C, top*, Western blots for CDK6 in original HCT-116 cells and HCT-116 cells transfected with miR-124a precursor, showing CDK6 down-regulation. RT-PCR analyses of CDK6 mRNA do not show any change. *Bottom*, Western blot for phosphorylated Rb shows that HCT-116 cells transfected with the miR-124a precursor, HCT-116 cells treated with the DNA-demethylating agent, and DKO cells are hypophosphorylated at the two Rb sites mediated by CDK6. *D*, immunohistochemistry of CDK6 and phosphorylated Rb in human primary lung tumors. *Left*, miR-124a unmethylated tumor showing loss of CDK6 expression and hypophosphorylated Rb; *right*, miR-124a methylated tumor showing strong CDK6 staining and phosphorylated Rb. Those tumors with a high percentage of tumor cells (>50%) with positive nuclear staining were considered to have strong CDK6 expression. *Bottom*, table representing the distribution of cases. *GAPDH*, glyceraldehyde-3-phosphate dehydrogenase.

Top, base pairing comparison between mature miR-124a and the wild-type (WT) or mutant (MUT) CDK6 putative target site. *Bottom*, luciferase assays of DKO (miR-124a expressor) or HCT-116 (miR-124a non-expressor) cells transfected with firefly luciferase constructs containing CDK6-WT or CDK6-MUT. In the case of HCT-116 cells, the results of miR-124a cotransfection are also shown. Normalized luciferase activities are represented. *C, top*, Western blots for CDK6 in original HCT-116 cells and HCT-116 cells transfected with miR-124a precursor, showing CDK6 down-regulation. RT-PCR analyses of CDK6 mRNA do not show any change. *Bottom*, Western blot for phosphorylated Rb shows that HCT-116 cells transfected with the miR-124a precursor, HCT-116 cells treated with the DNA-demethylating agent, and DKO cells are hypophosphorylated at the two Rb sites mediated by CDK6. *D*, immunohistochemistry of CDK6 and phosphorylated Rb in human primary lung tumors. *Left*, miR-124a unmethylated tumor showing loss of CDK6 expression and hypophosphorylated Rb; *right*, miR-124a methylated tumor showing strong CDK6 staining and phosphorylated Rb. Those tumors with a high percentage of tumor cells (>50%) with positive nuclear staining were considered to have strong CDK6 expression. *Bottom*, table representing the distribution of cases. *GAPDH*, glyceraldehyde-3-phosphate dehydrogenase.

Top, base pairing comparison between mature miR-124a and the wild-type (WT) or mutant (MUT) CDK6 putative target site. *Bottom*, luciferase assays of DKO (miR-124a expressor) or HCT-116 (miR-124a non-expressor) cells transfected with firefly luciferase constructs containing CDK6-WT or CDK6-MUT. In the case of HCT-116 cells, the results of miR-124a cotransfection are also shown. Normalized luciferase activities are represented. *C, top*, Western blots for CDK6 in original HCT-116 cells and HCT-116 cells transfected with miR-124a precursor, showing CDK6 down-regulation. RT-PCR analyses of CDK6 mRNA do not show any change. *Bottom*, Western blot for phosphorylated Rb shows that HCT-116 cells transfected with the miR-124a precursor, HCT-116 cells treated with the DNA-demethylating agent, and DKO cells are hypophosphorylated at the two Rb sites mediated by CDK6. *D*, immunohistochemistry of CDK6 and phosphorylated Rb in human primary lung tumors. *Left*, miR-124a unmethylated tumor showing loss of CDK6 expression and hypophosphorylated Rb; *right*, miR-124a methylated tumor showing strong CDK6 staining and phosphorylated Rb. Those tumors with a high percentage of tumor cells (>50%) with positive nuclear staining were considered to have strong CDK6 expression. *Bottom*, table representing the distribution of cases. *GAPDH*, glyceraldehyde-3-phosphate dehydrogenase.

Top, base pairing comparison between mature miR-124a and the wild-type (WT) or mutant (MUT) CDK6 putative target site. *Bottom*, luciferase assays of DKO (miR-124a expressor) or HCT-116 (miR-124a non-expressor) cells transfected with firefly luciferase constructs containing CDK6-WT or CDK6-MUT. In the case of HCT-116 cells, the results of miR-124a cotransfection are also shown. Normalized luciferase activities are represented. *C, top*, Western blots for CDK6 in original HCT-116 cells and HCT-116 cells transfected with miR-124a precursor, showing CDK6 down-regulation. RT-PCR analyses of CDK6 mRNA do not show any change. *Bottom*, Western blot for phosphorylated Rb shows that HCT-116 cells transfected with the miR-124a precursor, HCT-116 cells treated with the DNA-demethylating agent, and DKO cells are hypophosphorylated at the two Rb sites mediated by CDK6. *D*, immunohistochemistry of CDK6 and phosphorylated Rb in human primary lung tumors. *Left*, miR-124a unmethylated tumor showing loss of CDK6 expression and hypophosphorylated Rb; *right*, miR-124a methylated tumor showing strong CDK6 staining and phosphorylated Rb. Those tumors with a high percentage of tumor cells (>50%) with positive nuclear staining were considered to have strong CDK6 expression. *Bottom*, table representing the distribution of cases. *GAPDH*, glyceraldehyde-3-phosphate dehydrogenase.

Top, base pairing comparison between mature miR-124a and the wild-type (WT) or mutant (MUT) CDK6 putative target site. *Bottom*, luciferase assays of DKO (miR-124a expressor) or HCT-116 (miR-124a non-expressor) cells transfected with firefly luciferase constructs containing CDK6-WT or CDK6-MUT. In the case of HCT-116 cells, the results of miR-124a cotransfection are also shown. Normalized luciferase activities are represented. *C, top*, Western blots for CDK6 in original HCT-116 cells and HCT-116 cells transfected with miR-124a precursor, showing CDK6 down-regulation. RT-PCR analyses of CDK6 mRNA do not show any change. *Bottom*, Western blot for phosphorylated Rb shows that HCT-116 cells transfected with the miR-124a precursor, HCT-116 cells treated with the DNA-demethylating agent, and DKO cells are hypophosphorylated at the two Rb sites mediated by CDK6. *D*, immunohistochemistry of CDK6 and phosphorylated Rb in human primary lung tumors. *Left*, miR-124a unmethylated tumor showing loss of CDK6 expression and hypophosphorylated Rb; *right*, miR-124a methylated tumor showing strong CDK6 staining and phosphorylated Rb. Those tumors with a high percentage of tumor cells (>50%) with positive nuclear staining were considered to have strong CDK6 expression. *Bottom*, table representing the distribution of cases. *GAPDH*, glyceraldehyde-3-phosphate dehydrogenase.

Top, base pairing comparison between mature miR-124a and the wild-type (WT) or mutant (MUT) CDK6 putative target site. *Bottom*, luciferase assays of DKO (miR-124a expressor) or HCT-116 (miR-124a non-expressor) cells transfected with firefly luciferase constructs containing CDK6-WT or CDK6-MUT. In the case of HCT-116 cells, the results of miR-124a cotransfection are also shown. Normalized luciferase activities are represented. *C, top*, Western blots for CDK6 in original HCT-116 cells and HCT-116 cells transfected with miR-124a precursor, showing CDK6 down-regulation. RT-PCR analyses of CDK6 mRNA do not show any change. *Bottom*, Western blot for phosphorylated Rb shows that HCT-116 cells transfected with the miR-124a precursor, HCT-116 cells treated with the DNA-demethylating agent, and DKO cells are hypophosphorylated at the two Rb sites mediated by CDK6. *D*, immunohistochemistry of CDK6 and phosphorylated Rb in human primary lung tumors. *Left*, miR-124a unmethylated tumor showing loss of CDK6 expression and hypophosphorylated Rb; *right*, miR-124a methylated tumor showing strong CDK6 staining and phosphorylated Rb. Those tumors with a high percentage of tumor cells (>50%) with positive nuclear staining were considered to have strong CDK6 expression. *Bottom*, table representing the distribution of cases. *GAPDH*, glyceraldehyde-3-phosphate dehydrogenase.

Top, base pairing comparison between mature miR-124a and the wild-type (WT) or mutant (MUT) CDK6 putative target site. *Bottom*, luciferase assays of DKO (miR-124a expressor) or HCT-116 (miR-124a non-expressor) cells transfected with firefly luciferase constructs containing CDK6-WT or CDK6-MUT. In the case of HCT-116 cells, the results of miR-124a cotransfection are also shown. Normalized luciferase activities are represented. *C, top*, Western blots for CDK6 in original HCT-116 cells and HCT-116 cells transfected with miR-124a precursor, showing CDK6 down-regulation. RT-PCR analyses of CDK6 mRNA do not show any change. *Bottom*, Western blot for phosphorylated Rb shows that HCT-116 cells transfected with the miR-124a precursor, HCT-116 cells treated with the DNA-demethylating agent, and DKO cells are hypophosphorylated at the two Rb sites mediated by CDK6. *D*, immunohistochemistry of CDK6 and phosphorylated Rb in human primary lung tumors. *Left*, miR-124a unmethylated tumor showing loss of CDK6 expression and hypophosphorylated Rb; *right*, miR-124a methylated tumor showing strong CDK6 staining and phosphorylated Rb. Those tumors with a high percentage of tumor cells (>50%) with positive nuclear staining were considered to have strong CDK6 expression. *Bottom*, table representing the distribution of cases. *GAPDH*, glyceraldehyde-3-phosphate dehydrogenase.

Top, base pairing comparison between mature miR-124a and the wild-type (WT) or mutant (MUT) CDK6 putative target site. *Bottom*, luciferase assays of DKO (miR-124a expressor) or HCT-116 (miR-124a non-expressor) cells transfected with firefly luciferase constructs containing CDK6-WT or CDK6-MUT. In the case of HCT-116 cells, the results of miR-124a cotransfection are also shown. Normalized luciferase activities are represented. *C, top*, Western blots for CDK6 in original HCT-116 cells and HCT-116 cells transfected with miR-124a precursor, showing CDK6 down-regulation. RT-PCR analyses of CDK6 mRNA do not show any change. *Bottom*, Western blot for phosphorylated Rb shows that HCT-116 cells transfected with the miR-124a precursor, HCT-116 cells treated with the DNA-demethylating agent, and DKO cells are hypophosphorylated at the two Rb sites mediated by CDK6. *D*, immunohistochemistry of CDK6 and phosphorylated Rb in human primary lung tumors. *Left*, miR-124a unmethylated tumor showing loss of CDK6 expression and hypophosphorylated Rb; *right*, miR-124a methylated tumor showing strong CDK6 staining and phosphorylated Rb. Those tumors with a high percentage of tumor cells (>50%) with positive nuclear staining were considered to have strong CDK6 expression. *Bottom*, table representing the distribution of cases. *GAPDH*, glyceraldehyde-3-phosphate dehydrogenase.

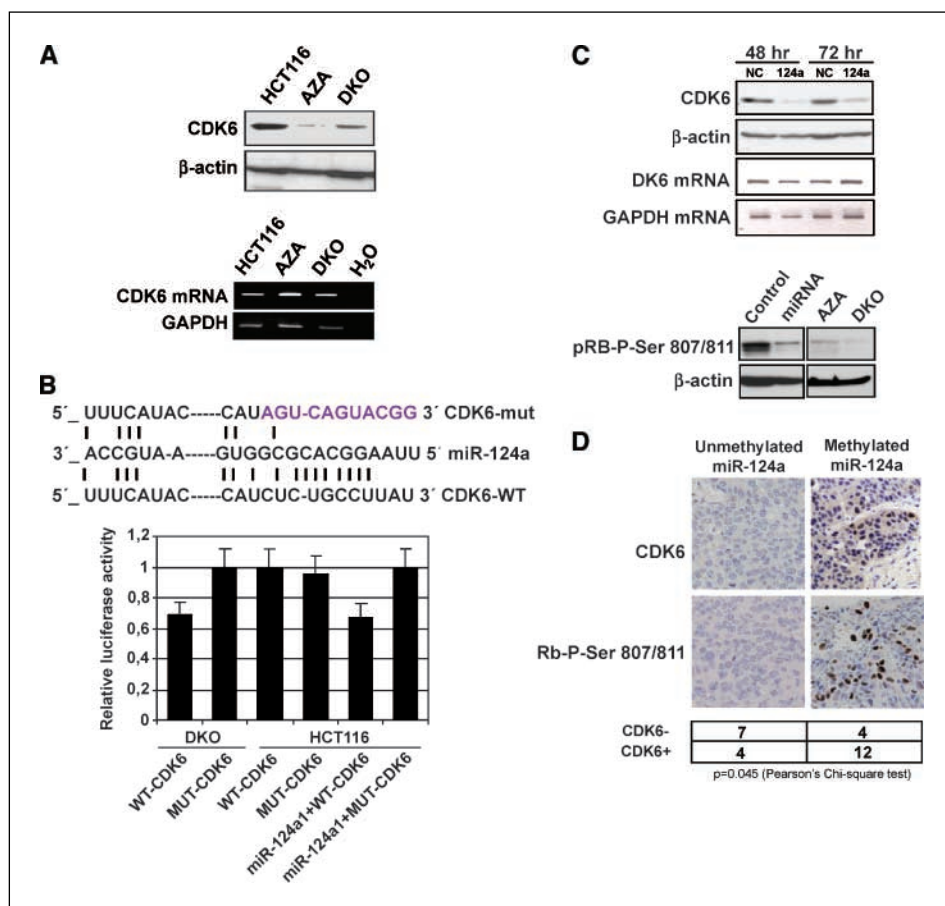


Table 1. Profile of miR-124a methylation in human cancer cell lines and primary tumors (Cont'd)

A.	Tissue (cell lines and control samples)																							
	Normal colon					Normal breast				Normal lung				Control										
	NC1	NC2	NC3	NC4	NC5	NC6	NC7	NC8	NC9	NC10	NB1	NB2	NB3	NB4	NLu1	NLu2	NLu3	NLu4	NL1	NL2	NL3	NL4	DKO	IVD
miR-124a1																								
miR-124a2																								
miR-124a3																								

CpG island was always unmethylated (Fig. 1B). In the case of miR124, this miRNA is represented in three genomic loci [miR-124a-1 (8p23.1), miR-124a-2 (8q12.3), and miR-124a-3 (20q13.33)], and in all cases, the corresponding CpG island was methylated in HCT-116 and unmethylated in normal colon (Fig. 1B; Supplementary Figs. S2 and S3).

The presence of miR-124a hypermethylation was not a feature of this particular cell line, but analyzing a comprehensive collection of human cancer cell lines ($n = 22$; Fig. 1C; Table 1A) and primary samples ($n = 171$; Fig. 2; Table 1B) from colon, breast, and lung carcinomas, leukemias, and lymphomas also showed a frequent presence of miR-124a hypermethylation. In the case of primary colorectal tumors, miRNA-124a hypermethylation was observed in 75% (42 of 56) of patients (Fig. 2, *top*; Table 1B). miRNA-124a methylation was also confirmed by bisulfite genomic sequencing of selected cases (Supplementary Fig. S3). However, miR-124a methylation was absent in neuroblastoma and sarcoma cell lines ($n = 7$; Fig. 1C; Table 1A) and primary tumors ($n = 37$; Fig. 2; Table 1B). Thus, miR-124a became our prime candidate for a hypermethylation/cancer-specific event.

Epigenetic repression of miR-124a in cancer cells. To effectively show the epigenetic silencing of miR-124a in cancer cells, we first mapped by RACE the transcriptional start site of miR-124a, and it was found indeed in the analyzed CpG island (Fig. 1A). Most important, RT-PCR analyses showed that precursor and mature miR-124a expression was absent in HCT-116 cells with CpG island hypermethylation and restored in HCT-116 cells treated with the DNA-demethylating agent and in DKO cells (Fig. 1D). The association between miR-124 methylation and loss of expression was also found in cancer cell lines from other tumor types (Fig. 1D). Because DNA methylation silencing is closely linked to histone modifications to determine active versus inactive gene expression, we analyzed by chromatin immunoprecipitation the histone modification pattern and the binding of the transcriptional repressors methyl-CpG-binding domain proteins (MBD; ref. 17) to the miR-124a CpG island. miR-124a CpG island hypermethylation was accompanied by the absence of histone modification marks associated with gene activation, such as histone H3 and H4 acetylation and trimethylation of Lys⁴ of histone H3, and occupancy by MBDS, such as MeCP2 and MBD2 (Fig. 1D). The induction of miR-124a CpG island DNA hypomethylation events by the demethylating agent or in DKO cells was associated with the emergence of histone marks of active transcription and release of binding by MBDS (Fig. 1D).

miR-124a epigenetic silencing mediates CDK6 activation and Rb phosphorylation. To determine whether the epigenetic silencing of miR-124a had functional cancer relevance to escape the putative tumor suppressor function of miR-124a, we examined its effect in the regulation of presumed target genes with oncogenic capacity. Using computational prediction for miR-124a target genes, we observed that CDK6 was one of the best potential targets for miR-124a. CDK6 is involved in cell cycle progression and differentiation (17), and it constitutes an attractive target for the development of anticancer compounds (18). Using CDK6 Western blot analyses, we observed that whereas the original HCT-116 cells with miR-124a methylation-associated silencing strongly expressed CDK6, the cells treated with the demethylating agent or the DKO cells showed CDK6 down-regulation (Fig. 3A). On the other hand, there was no difference in the CDK6 mRNA expression levels in any of the described cells (Fig. 3A), suggesting translational inhibition of CDK6 by miR-124a, rather than mRNA degradation or transcriptional repression. Most important, a functional link was established by performing a luciferase reporter assay with a vector containing the CDK6 wild-type (WT) putative 3'-UTR target site and a mutant form (MUT), in different contexts of miR-124a expression. Luciferase activity of miR-124a-expressing DKO cells transfected with CDK6-WT was significantly lower than DKO cells transfected with CDK6-MUT ($P = 0.031$). In contrast, the luciferase activities of miR-124a non-expressing HCT-116 cells transfected with CDK6-WT and CDK6-MUT showed no measurable differences (Fig. 3B). However, when we co-transfected miR-124a, luciferase activity of HCT-116 CDK6-WT-transfected cells was significantly lower than CDK6-MUT ($P = 0.002$; Fig. 3B).

To further confirm the targeting of CDK6 by miR-124a, HCT-116 cells were transfected with miR-124a precursor molecules, which are designed to mimic endogenous miR-124a and directly enter the miRNA processing pathway. Overexpression of miR-124a induced a reduction of CDK6 protein level (Fig. 3C). Most important, the miR-124a transfection diminished the phosphorylation of Rb in the residues 807 and 811, the targets of CDK6 (17). The induction of endogenous miR-124a in HCT-116 cells by the demethylating drug or in DKO cells also reduced Rb phosphorylation (Fig. 3C). Remarkably, an immunostaining analyses of CDK6 expression in lung cancer patients ($n = 27$) showed that miR-124a hypermethylation was associated with strong expression of CDK6 and Rb phosphorylation ($P = 0.045$, Pearson's χ^2 test; Fig. 3D). All these data indicate that CDK6 is targeted by miR-124a, and that epigenetic silencing of miR-124a in cancer cells leads to CDK6 up-regulation.

In summary, we have shown that one mechanism accounting for the observed down-regulation of miRNAs in human cancer is CpG island hypermethylation, in a similar manner that it is now well accepted for classic tumor suppressor genes. We provide an illustrative example in colon cancer with the epigenetic silencing of miR-124a and its functional consequences for CDK6 activity. Most important, miR-124a function can be restored by erasing DNA methylation, in a similar scenario that it has been shown for miR-127 and its target BCL6 (6). Thus, the epigenetic dysregulation of miRNAs in human cancer (19) constitutes an emerging scientific

field that may have significant consequences for cancer patients undergoing treatment with DNA-demethylating drugs in the clinical arena.

Acknowledgments

Received 11/17/2006; revised 12/20/2006; accepted 1/3/2007.

The costs of publication of this article were defrayed in part by the payment of page charges. This article must therefore be hereby marked *advertisement* in accordance with 18 U.S.C. Section 1734 solely to indicate this fact.

References

1. He L, Hannon GJ. MicroRNAs: small RNAs with a big role in gene regulation. *Nat Rev Genet* 2004;5:522–31.
2. Miska EA. How microRNAs control cell division, differentiation and death. *Curr Opin Genet Dev* 2005;5: 563–8.
3. Lu J, Getz G, Miska EA, et al. MicroRNA expression profiles classify human cancers. *Nature* 2005; 435:834–8.
4. Johnson SM, Grosshans H, Shingara J, et al. RAS is regulated by the let-7 microRNA family. *Cell* 2005;120: 635–47.
5. Cimmino A, Calin GA, Fabbri M, et al. miR-15 and miR-16 induce apoptosis by targeting BCL2. *Proc Natl Acad Sci U S A* 2005;102:13944–9.
6. Saito Y, Liang G, Egger G, et al. Specific activation of microRNA-127 with downregulation of the proto-oncogene BCL6 by chromatin-modifying drugs in human cancer cells. *Cancer Cell* 2006;9:435–43.
7. Thomson JM, Newman M, Parker JS, Morin-Kensicki EM, Wright T, Hammond SM. Extensive post-transcriptional regulation of microRNAs and its implications for cancer. *Genes Dev* 2006;20:2202–7.
8. Costello JF, Plass C. Methylation matters. *J Med Genet* 2001;38:285–303.
9. Esteller M. CpG island hypermethylation and tumor suppressor genes: a booming present, a brighter future. *Oncogene* 2002;21:5427–40.
10. Herman JG, Baylin SB. Gene silencing in cancer in association with promoter hypermethylation. *N Engl J Med* 2003;349:2042–54.
11. Rhee I, Bachman KE, Park BH, et al. DNMT1 and DNMT3b cooperate to silence genes in human cancer cells. *Nature* 2002;416:552–6.
12. Miska EA, Alvarez-Saavedra E, Townsend M, et al. Microarray analysis of microRNA expression in the developing mammalian brain. *Genome Biol* 2004;5:R68.
13. Paz MF, Wei S, Cigudosa JC, et al. Genetic unmasking of epigenetically silenced tumor suppressor genes in colon cancer cells deficient in DNA methyltransferases. *Hum Mol Genet* 2003;12:2209–19.
14. Takai D, Jones PA. The CpG island searcher: a new WWW resource. *In Silico Biol* 2003;3:235–40.
15. Shi R, Chiang VL. Facile means for quantifying microRNA expression by real-time PCR. *BioTechniques* 2005;39:519–25.
16. Ballestar E, Paz MF, Valle L, et al. Methyl-CpG binding proteins identify novel sites of epigenetic inactivation in human cancer. *EMBO J* 2003;22:6335–45.
17. Gossel MJ, Hinds PW. Beyond the cell cycle: a new role for Cdk6 in differentiation. *J Cell Biochem* 2006;97: 485–93.
18. Hirai H, Kawanishi N, Iwasawa Y. Recent advances in the development of selective small molecule inhibitors for cyclin-dependent kinases. *Curr Top Med Chem* 2005; 5:167–79.
19. Saito Y, Jones PA. Epigenetic activation of tumor suppressor microRNAs in human cancer cells. *Cell Cycle* 2006;5.

Correction: Multiple Properties of E6 Contribute to Cervical Cancer

In the article on how multiple properties of E6 contribute to cervical cancer in the February 15, 2007 issue of *Cancer Research* (1), the grant support should have appeared in the Acknowledgments section as follows:

Grant support: Grants CA098428, CA022443, CA014520, and CA009135 from the NIH.

1. Shai A, Brake T, Somoza C, Lambert PF. The human papillomavirus E6 oncogene dysregulates the cell cycle and contributes to cervical carcinogenesis through two independent activities. *Cancer Res* 2007;67:1626–35.

Cancer Research

The Journal of Cancer Research (1916–1930) | The American Journal of Cancer (1931–1940)

Genetic Unmasking of an Epigenetically Silenced microRNA in Human Cancer Cells

Amaia Lujambio, Santiago Ropero, Esteban Ballestar, et al.

Cancer Res 2007;67:1424-1429.

Updated version	Access the most recent version of this article at: http://cancerres.aacrjournals.org/content/67/4/1424
Supplementary Material	Access the most recent supplemental material at: http://cancerres.aacrjournals.org/content/suppl/2007/02/15/67.4.1424.DC1

Cited articles	This article cites 17 articles, 4 of which you can access for free at: http://cancerres.aacrjournals.org/content/67/4/1424.full#ref-list-1
Citing articles	This article has been cited by 73 HighWire-hosted articles. Access the articles at: http://cancerres.aacrjournals.org/content/67/4/1424.full#related-urls

E-mail alerts	Sign up to receive free email-alerts related to this article or journal.
Reprints and Subscriptions	To order reprints of this article or to subscribe to the journal, contact the AACR Publications Department at pubs@aacr.org .
Permissions	To request permission to re-use all or part of this article, use this link http://cancerres.aacrjournals.org/content/67/4/1424 . Click on "Request Permissions" which will take you to the Copyright Clearance Center's (CCC) Rightslink site.